MAE 6900 Special Investigations in Mechanical and Aerospace Engineering

Masters of Engineering Degree (Aerospace)

Granular Dynamics of Non-Spherical Particles

Y. Clement Ng

NetID: ycn3

Report Date: May 15, 2014

Professor: Olivier Desjardins

Sibley School of Mechanical and Aerospace Engineering

Cornell University

Abstract

Masters of Engineering Degree (Aerospace)

Project Title:

Granular Dynamics of Non-Spherical Particles

Author:

Y. Clement Ng

Abstract:

This research project in the Computational Thermo-Fluids Laboratory analyzes the granular dynamics of non-spherical particles in a fluidized bed reactor. Current computational models of this multiphase particle-laden flow classically assume spherical particles. A literature review of drag correlations for non-spherical shapes was studied. The effective diameter and shape factor of arbitrary particles nondimensionally quantify particles shapes for numerical analysis.

This project adapts the developed NGA research code to represent the particles as a collection of overlapping spheres. Modeling collisions using the soft sphere model, a pseudo three-dimensional setup uses two-sphere fluid particles to simulations the intermolecular and intramolecular interactions of dense particle-laden flow. The effects of particle shape and flow dynamics are examined to determine the mixing quality.

Overview

This project analyzes the models of non-spherical particles in a fluidized bed through a computational simulation using NGA code. The multiphase flow problem can be classified as a two-phase solid-liquid flow. The particle-laden flow considers various particles under sustained contact in a dispersed phase and a flowing gas in a continuous or carrier phase.

Current computational models are typically limited to spherical models for simplicity. In practice, particles form arbitrary, non-uniform shapes that are elongated and deformed. These irregularly shaped particles are found in industrial processes. Fluidized beds, slurry pipes, spouted beds, and sludge settling all involve chemical engineering processes where liquid or gas fluids turbulently mix densely-packed solid particles. By modeling the solid particles more accurately as they exist in these processes, the dynamics and mixing effects can be represented more accurately in determining the effectiveness of the overall geometry. The representation using non-spherical particles can be extended to other applications that involve diatomic or polyatomic molecules. Chemical reactions and combustion processes depend on these intermolecular collisions and often involve numerous species of various shapes.

The particle shape can be classified with non-dimensional parameters to compare the relative geometries of spheres and other elongated shapes. With a particle volume V, the nominal diameter is defined as

$$d_n = \left(\frac{6V}{\pi}\right)^{\frac{1}{3}}$$

and the surface equivalent sphere diameter is defined as

$$d_A = \sqrt{\frac{4A_p}{\pi}}$$

where A_p is the projected area of the equivalent sphere. The ratio of these two diameters is the equivalent volume particle $\frac{d_A}{d_n}$. The particle's sphericity is defined as

$$\varphi = \frac{\pi d_n^2}{A}$$

where A is its surface area. These two non-dimensional numbers compares the roundness of an ellipsoid to that of a smooth sphere. For the fluid, the Reynolds Number Re classifies the type of flow. For the multiphase flow, the volume fraction of particles ε_p defines the amount of particles per unit volume. Likewise the volume fraction of fluid ε_f defines the amount of fluid per unit volume. These two volume fractions are related by the following equation.

$$\varepsilon_f = 1 - \varepsilon_p$$

Since only fluid and particles exist in the domain, their volume fractions sum to unity.

The results of the particle mixing and dynamics are described with additional parameters. The effect of the fluid on the particles is characterized by their drag coefficients C_D. This dimensionless variable is a function of the particle shape and has many correlations that are developed a posteriori. For systems with two types of particles, the Lacey mixing index M is:

$$M = \frac{\sigma_0^2 - S^2}{\sigma_0^2 - \sigma_r^2}$$

where σ_0^2 is the variance of a fully segregated mixture, σ_r^2 is the variance of a completely random mixture, and S^2 is the variance of the mixture in consideration. Starting from a fully segregated mixture ($M = 0$), the flow gradually agitates the mixing quality until $M \rightarrow 1$. For flow to be able to mix particles, the fluid velocity must be at least the minimum spouting velocity u_{ms}. The fluid velocity is often expressed as a ratio of the minimum spouting velocity. Effective mixing occurs at values just above this minimum.

Project Objectives

A computational model will be developed using NGA code. From its description, "NGA is large-eddy simulation (LES) and direct numerical simulation (DNS) code capable of solving the low-Mach number variable density Navier-Stokes equations on structured Cartesian and cylindrical meshes. It features a range of models and methods designed for solving multiphase reacting turbulent flows in complex geometries." Current computational models of this multiphase particle-laden flow classically assume spherical particles. This project adapts the developed NGA code to represent the particles as a collection of overlapping spheres. Multiple simulations of the intermolecular and intramolecular interactions will determine the effects of particle shape on granular dynamics. A high performance computer will be needed to compile the code.

Finally, the non-spherical simulation results will be compared with those of the reference spherical model to observe and quantify the differences. The non-sphericality effects on the overall flow field will be analyzed. Particle spacing and clumping effects will also be compared between both cases. If there is time, additional differences, such as wall effects and the collisions models, will be quantified. Similarly, different, non spherical particles can also be considered. This analysis step will conclude with a final presentation and paper of the results.

The project also reviews the work of other researchers in this field. A literature review was conducted to analyze the accomplishments of previous works. A paper critique of Ren's article in 2012 further analyzed the methods and results of a computational simulation of corn-shaped particles in a spouted bed. These two papers structure the framework and direction of this project.

Literature Review

This project extends the gas-solid particle-laden flow simulations carried out by the Computational Thermo-Fluids Laboratory at Cornell University. The study analyzes the framework for modelling polydisperse flows in applications such as fluidized bed reactors and spouted fluidization. Capecelatro models the solid particles in a Lagrangian frame and the gas flow in an Eulerian frame. Using this approach combined with volume filtering, the Eulerian cell size can be smaller than the Lagrangian particles to allow mesh refinement. In verification simulations, the Reynolds number ranged from 300 to above 13000. The inter-particle interaction is modelled using the soft-sphere approach. In this method, a collision between two spherical particles results an unsticking force modeled by spring and damper connections. The collision force is activated with a radius of influence as determined by the Courant-Friedrichs-Lewy (CFL) stability condition.

However, the boundary condition are assumed with wall collisions modelled as infinitely small wall particles with zero radius and infinite mass. The particle-wall interaction is outside the scope of study of this project. Using NGA code, the study by Capecelatro scaled up to 4096 cores on National Renewable Energy Laboratory's (NREL) high performance computers with good results using message passing interface (MPI). Because change the particle shape should change the efficiency significantly, and because the scale of this project is much smaller, the efficiency of the code will not be investigated. For the project, the approach will the similar to that of Capecelatro. The verification of the non-spherical model will be compared against the spherical model and experimental results.

Although it does not focus on non-spherical particles in particular, a recent article by Subramaniam summarizes the field of Lagrangian-Eulerian methods for multiphase flows. This review article provides a fundamental understanding of this type of flow. It also covers the modelling of such particles, its challenges, and multiple submodels that each cover specific flow features.

The NGA code developed by Desjardins uses a high order conservative finite difference scheme based on Morinishi. It provides a means to simulate variable density, reactive turbulent flows using direct numerical simulation (DNS) and large eddy simulation (LES) methods. The code supports Cartesian and cylindrical coordinate systems with variable mesh sizes. Mass, momentum, and energy are conserved to provide accurate solutions, and viscous effects are modelled. Care is taken for boundary conditions at the walls and for the singularity as $r \to 0$ in cylindrical coordinates on conservation equations. The code is limited to low-Mach number regimes, but such speeds are sufficient for practical applications of a fluidized bed reactor as in this project. NGA has been verified in typical canonical flows, including homogenous isotropic turbulence, vortex ring colliding with a wall, the Rayleigh-Taylor instability, turbulent pipe, and round jets. Thus, it should be suitable for applications in this project. For many simulations in other articles, the discrete element method (DEM) was used to model the behavior of the particles. Beestra instead uses a lattice-Boltzmann code for their simulation. Generally, all simulations have good agreement with their respective experimental tests to confirm the validity of the data.

A number of reference articles have considered irregularly shaped particles of various geometries. The most common is in the shape of ellipsoids, elongations of spheres in multiple aspect ratios, as simulated by Donev and Zhou. Such methodology is sensible and well approximates the shape of particles in industrial processes. Zhong has modeled the flow of cylinder-shaped particles the length of 3 spheres using DEM and has conducted experiments for verification. However, there is limited data on their results and conclusions of the model's accuracy in hydrodynamics. Most interestingly, Ren simulated corn-shaped particles in a spouted bed using DEM. This article is most similar to the conditions of this project in terms of the particle shape, but differs slightly in the container shape. The corn particle is modeled using a multi-sphere method represented geometrically by four overlapping spheres (see Fig 1 of the article). The results of this method analyzes the effects of particle shape, particle density, spouting gas velocity of corn particles. Additionally, binary particles systems of spherical and corn-shape particles are considered in the mixing process. This project can follow the simulation procedure of Ren, but with a dumbbell-shaped particle. However, there seems to be no experimental verification of the corn-shaped particles in their paper with a physical setup or industrial spouted bed applications. For dumbbell-shaped particles as considered in the project, there exists limited data of this choice of particle shape. An older 2D simulation by Allen has surveyed non-spherical shapes, including lines, ellipsoids, spherocylinders, and dumbbells. This project will analyze dumbbell shapes formed by two overlapping spheres in a 3D case.

Experimental data of non-spherical particles range from arbitrary polydisperse shapes as found in real applications to specific studies on particles created from tangent spheres. Hottovy has experimentally tested the drag coefficients for irregularly shaped solid particles of similar particle diameter. Chien has experimentally classified the settling velocity of irregularly shaped particles in Newtonian and non-Newtonian flows. In both cases, particles do not follow a specific shape; they vary greatly in shape factor values. Tran-Cong has experimentally determined the drag coefficients of particles created by gluing glass spheres in a laboratory. Six shapes were investigated: close-to-sphere, pyramid, star, H-shaped, Crosse-shaped, and cylindrical bar. The star, H-shaped, and Crosse shaped particles are more similar to the dumbbell shape, although the H-shaped and Crosse-shapes are only features in two dimensions. The factors contributing to the drag coefficient include the nominal diameter, ratio of surface-equivalent-sphere to the nominal diameter, and particle circularity factor. These measure characterize the deviation from the spherical properties. These shape factors and geometric parameters define the dynamics of fluidized bed flows, including its porosity and its pressure gradients as shown by Hilton. While a number of shapes have been presented here, the lack of dumbbell-shaped particles as a model for particle-laden flows does not restrict this project to shapes already studied. While the dumbbell model cannot be directly verified against or derived from an identical experiment, this project can compare the characteristics on the flow with that in the articles above, and also verify the accuracy of NGA for non-sphericity. Conversely, the existence of a simulation with dumbbell-shaped particles can lead to the experimental conduction of a dataset in the future that will verify the model's accuracy.

Drag Correlations

Particle shapes can be classified into two sets of categories: spherical versus non-spherical, and regular versus irregular. Spherical shapes have uniform, nearly-circular cross sections. Non-spherical shapes have additional secondary motions and transverse lift forces dependent on the particle orientation. Most historically established research focuses on regularly shaped particles for its reproducible results. However, practical applications use irregularly shaped, non-spherical particles, such as pulverized biomass, flakes, and agglomerates. Goosens, Hottovy, and Loth have studied such irregularly shaped particles. To quantify non-spherical particles, the equivalent diameter is defined for the length dimension. The equivalent diameter can be defined using projected area, mean chord length, density, terminal velocity, surface area, or volume equivalent to their respective spheres with the same values. The definition selection is dependent on the applications and proposed correlations. Alternatively, the particle shape can classified using shape factors. Four major shape factors are identified: Corey shape factor, volumetric shape factor, roundness, and sphericity. The standard parameter choice to express shape factor is sphericity ϕ, which is defined as the ratio of the surface of a sphere with the same volume as the particle and the surface area of the actual particle. This parameter has become the popular choice for its simplicity to quantify the shape of arbitrary particles. Thus, correlations for coefficient of drag are functions of only two parameters, Reynolds number and sphericity, where $C_D = C_D(Re, \phi)$.

Two reviewed articles have classified the status and progress of research in non-sphericity. In 1998, Chhabra compared five well-established drag correlations against 19 experimental data sets. The data ranges the entire regime of flow speeds from creeping Stokes flow to full turbulent, high Reynolds number flows. Correlations by Haider and Levenspiel, Ganser, Chien, Hartman, and Swamee and Ojha are analyzed. The compared experiments tested a variety of plates, discs, cylinders, cones, and other shapes. In general, the correlation by Ganser provided the best consistency across all data sets. He defines the drag correlation as

$$\frac{C_D}{K_2} = \frac{24}{ReK_1K_2}\left(1 + 0.1118(ReK_1K_2)^{0.6567}\right) + \frac{0.4305}{1 + \frac{3305}{ReK_1K_2}}$$

where K_1 is the Stokes' shape factor and K_2 is the Newton's shape factor. For non-spherical particles, the shape factors are

$$K_1 = \left(\frac{d_n}{3d} + \frac{2}{3}\phi^{-0.5}\right)^{-1} \qquad K_2 = 10^{1.8148(-\log\phi)^{0.5743}}$$

where $\frac{d_n}{d}$ is the effective diameter. Thus, both shape factors K_1 and K_2 are functions of sphericity only. This correlation has an average error of 16.3% and a maximum error of 181% for Lasso and Weidman's experiments using hollow cylinders and agglomerates. Chien propose a drag correlation as

$$C_D = \frac{30}{Re} + \frac{67.289}{e^{5.030\phi}}$$

which is valid for the range $0.2 \leq \phi \leq 1.0$. More recently in 2010, Mondo also considered the effects of secondary motion, orientation of particles relative to the flow, and turbulence interaction effects in addition to revisiting Chhabra's analysis of drag correlations. The general trade is that the correlations perform worse as the particles deviate from the ideal spherical shape. Mondo also admits that the best result for a specific shape is to make an empirical fit as a function of Reynolds number. However, this practically is not possible for every particle shape and application.

Typical particle shapes studied in simulations for non-spherical particles include cylinders, disks, and ellipsoids. However, the two overlapping spheres studied for this MEng project has rarely been studied because of its more complicated geometry. This shape may be named as sphere conglomerates or sphere clusters. Lasso and Weidman have studied drag on hollow cylinders and conglomerates, but only in the Stokes flow regime. The correlation proposed by Tran-Cong is based on Clift where

$$C_D = \frac{24}{Re}\frac{d_A}{d_n}\left[1 + \frac{0.15}{\sqrt{c}}\left(\frac{d_A}{d_n}Re\right)^{0.687}\right] + \frac{0.42\left(\frac{d_A}{d_n}\right)^2}{\sqrt{c}\left[1 + 4.25 \times 10^4\left(\frac{d_A}{d_n}Re\right)^{-1.16}\right]}$$

$\frac{d_A}{d_n}$ is the shape factor ratio and c is the particle circularity. The range of validity for this correlation is $0.15 < Re < 1500$, $0.80 < \frac{d_A}{d_n} < 1.50$, and $0.4 < c < 1.0$, which covers many engineering applications. As Reynolds number increases towards the range of $Re \to 1500$, the error is up to 20%. By using two parameters to define the shape factor, the six investigated shapes (close-to-sphere, pyramid, star, H-shaped, Crosse-shaped, and cylindrical bar) can be distinguished. Tran-Cong's correlation has been recently used by Crowe and Loth, the latter of which shows that the correlation equation collapses well for these normalized parameters.

To account for the orientation of the particle, Hölzer proposes a new "simple" correlation formula based on the work of Leith, Tran-Cong, and many other previous works. The correlation combines two terms for the Stokes regime with a correlation at high Reynolds numbers.

$$C_D = \frac{8}{Re}\frac{1}{\sqrt{\phi_{\parallel}}} + \frac{16}{Re}\frac{1}{\sqrt{\phi}} + \frac{3}{\sqrt{Re}}\frac{1}{\phi^{\frac{3}{4}}} + 0.4210^{0.4(-\log\phi)^2}\frac{1}{\phi_{\perp}}$$

Hölzer accounts for the particle orientation through distinguishing sphericity into the lengthwise sphericity $\phi_{\parallel}$ and the crosswise sphericity $\phi_{\perp}$. This correlation resolves the limitations of Leith with orientation dependent parameters and the limitation of Tran-Cong with a larger range of flow applicability. For the tested non-spherical particles, the correlation has an average error of 14.1% and a maximum error of 88%. Hölzer even argues that this correlation for drag coefficient is the most exact of arbitrary shaped particles since its proposal in 2008. Since then, this correlation has been used in simulations by Hilton in pneumatic conveying and fluidized bed applications to model the dynamics accurately.

Four commonly used drag correlations for non-spherical and irregular particles of varying complexity are presented. The accuracy of each correlation is also explored. The trend of correlation accuracy improves over time as research build upon previous works. Beginning with simple models, Ganser proposed a correlation that works well for only certain types of standard non-spherical particles. Work on particle cluster is first studied in the creeping flow regime. Chien and Tran-Cong each propose newer correlations based on their experimental results on irregular particles and particle clusters, respectively. Most recently, Hölzer suggests a simple formulation for the coefficient of drag that is accurate among a large range of Reynolds numbers and particle shapes. These drag correlations are used in simulations to calculate particle motion in industrial applications, such as of multiphase gas-solid flows in fluidized bed reactors.

Simulation Method

The multiphase flow problem for this project is simulated using an Euler-Lagrange methodology. The governing equations for the carrier and dispersed phase are as follows and are described in detail in the course lectures notes and by Capecelatro. For the fluid phase, continuity is conserved:

$$\frac{\partial \rho_f}{\partial t} + \nabla \cdot \left(\rho_f \vec{u}_f\right) = 0$$

where ρ_f is fluid density and $\vec{u}_f$ is the fluid velocity at each location in the domain. The conservation of momentum is given by:

$$\frac{\partial}{\partial t}\left(\rho_f \vec{u}_f\right) + \nabla \cdot \left(\rho_f \vec{u}_f \otimes \vec{u}_f\right) = \nabla \cdot \vec{\vec{\tau}} + \rho_f \vec{g}$$

where $\vec{\vec{\tau}}$ is the fluid stress tensor and $\vec{g}$ is gravity. The fluid stress tensor $\vec{\vec{\tau}}$ comprises of the pressure component p and dynamic viscosity μ.

The particle dynamics is described with translation and rotation motion. Linear momentum balance of forces show that:

$$m_p \frac{d\vec{u}_p}{dt} = \vec{f}_p^{inter} + \vec{F}_p^{col} + m_p \vec{g}$$

where m_p is particle mass, $\vec{f}_p^{inter}$ is the particle-fluid interaction force, and $\vec{F}_p^{col}$ is the particle-particle collision force. Angular momentum balance of the particle gives:

$$I_p \frac{d\vec{\omega}_p}{dt} = \int_{S_p} \frac{d_p}{2} \vec{n} \times (\vec{\tau} \cdot \vec{n})\, d\vec{y} + \sum_j \frac{d_p}{2} \vec{n} \times f_{t,j\to p}^{col}$$

where I_p is the particle moment of inertia, d_p is the particle effective diameter, and $f_{t,j\to p}^{col}$ is the tangential collision force between particles j and p.

The particle collision model uses the soft sphere approach as described in Capecelatro and shown in Figure 1. When two particles collide, a spring-mass-damper system is imposed for the normal component $f_{n,j\to p}^{col}$ of the interparticle force, and frictional forces are imposed for the tangential component $f_{t,j\to p}^{col}$. Both combine to create the overall collision force $\vec{F}_p^{col}$ to create velocity and angular velocity changes.

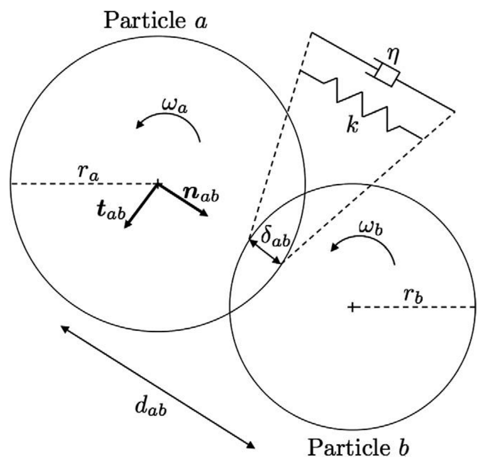

Figure 1: Soft sphere model

Spheres of the same pair do not undergo this collision model since they together represent a non-spherical particle.

The problem is solved in a two-dimensional domain with a pseudo-third z dimension. As shown in Figure 2, the fluidized bed has geometry 0.0128 x 0.0064 x $4 * 10^{-4}$ in the x, y, and z directions respectively. The fluid inlet flows from the "bottom" negative x boundary. On the "side" y boundaries, periodic boundaries create a continuous domain. Particles leave the periodic boundaries on one side and reappear on the opposite side. A bounded top exists on the positive x boundary. This domain is split into 32 x 16 x 1 cells in the x, y, and z directions respectively. The number of cells can be increased for mesh refinement.

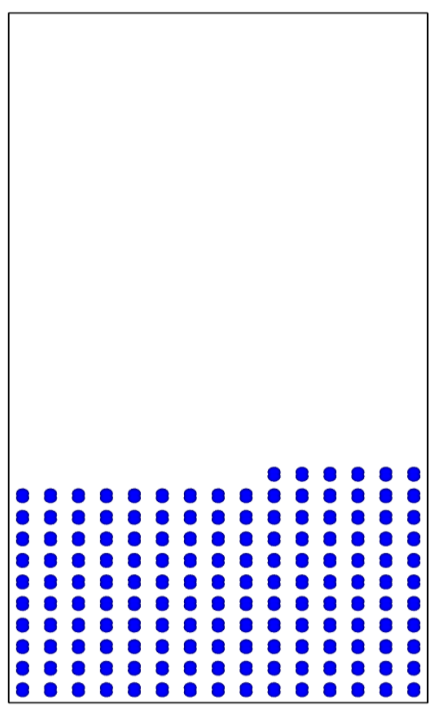

Figure 2: Initial Condition

The particles have a mean diameter of $200 * 10^{-6}$ and a spacing of $80 * 10^{-6}$. The volume fraction ε_p parameter determines the number of particles and is varied from 0.1 to 0.4. The inlet velocity was varies from below u_{ms} to values above u_{ms} that results in active mixing.

Results

A number of simulation cases were run by varying the input parameters. The NGA code has been validated with a number of classical models. Thus, it is assumed that the underlying code and governing equations accurately model physics of multiphase flows. As a result, only the particular case of this project needs validation. A basic run with inlet velocity $u << u_{ms}$ results in Figure 3.

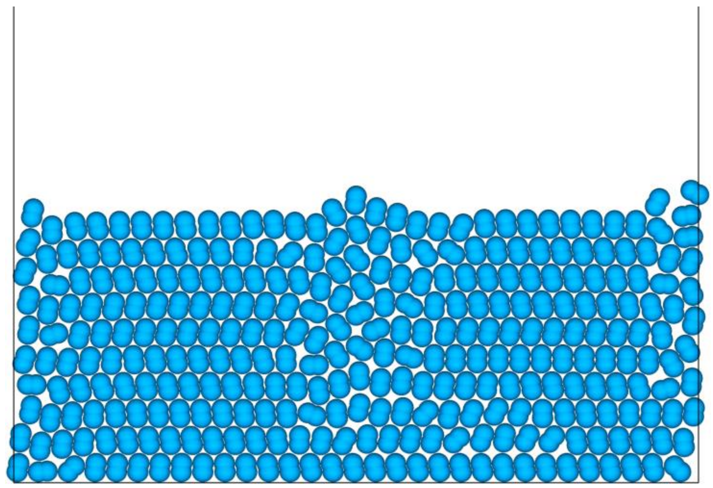

Figure 3: Verification

This verifies the proper boundary conditions where the bottom boundary contains the particles and the side boundaries provide a continuous and periodic boundary. The particles on the right edge interact with the particles on the left edge in the same manner as any other particle interaction in the middle. The selected soft sphere model is applied correctly. Gravity acts correctly based on the pressure distribution.

The simulation time step was set to $1 * 10^{-5}$ s. Large time steps created unphysical motions where particles leave the domain or where spheres of a pair separate when undergoing large collisional forces. This was also verified by satisfying the CFL condition for all time step calculations.

Discussion

The results are dependent on several input parameters. Animations and additional figures are presented in the Final Presentation to visualize these effects. By varying parameters such as inlet fluid velocity or particle volume fraction, the particle velocity, mixing quality, and angular velocity change significantly. Increasing the inlet fluid velocity increases the rate of mixing quality. Likewise, the number of collisions increased due to higher velocity and angular velocity components. The axial distribution is spread over a higher range as the particles fly higher. Further increasing inflow fluid velocity forces some particles to collide with the bounded top. Excessive fluid velocity causes particles to “float” and stay near the top boundary. Both of these phenomena are nonphysical. Conversely, fluid velocity below u_{ms} is insufficient to create mixing flow. Thus, the appropriate range of fluid velocities create optimum mixing conditions. Extreme values create other effects undesirable for industrial processes.

The particle spacing as determined by the volume fraction and bed height initializes the number of particles in the domain. Lowered volume fraction significantly decreases the computational time. However, the particle-laden flow no longer is truly dense. Increasing volume fraction is limited by overlapping particles in the initial condition, which adds nonphysical energy to the system according to the soft sphere model. Uniform spacing is less efficient than close packing, so the true maximum volume fraction is not achieved at the initial state.

The initial condition for the particles start stacked one on top another based on uniform spacing. This spacing creates the arrangement shown in Figure 3 where the central particles have the same identical orientation. In practice as shown by Hottovy, particles without being agitated are already mixed in random orientations. Such uniform initial condition creates the effects shown within the first second of the simulation. After this time period, the particles are approximately well mixed. However, if the initial distribution of particles was random, the simulation would more accurately represent the initial stages of mixing.

Interesting results occur from the selected geometrical modeling of the problem. The two-dimensional problem hides the dynamics from the third dimension. Particles lose a dimension of interaction. In addition, they cannot be packed as close as that in three dimensions. As a result, collisions occur more frequently than a three-dimensional simulation. Another observation from these simulations is that some particles become trapped in certain locations. These typically occur near the bottom boundary where the inlet flow and the particles above prevent effective mixing. This effect is undesirable in fluidized bed combustion where these particles will create uneven heating and reaction rates. Finally, it is assumed that the geometry is sufficiently large since periodic boundary conditions as implemented. While industrial reactors are very large on the scale of meters, they do have finite walls. Such effects are ignored here and can be considered with wall functions and modeling.

Increased mesh refinement of the Eulerian grid will accurately define the fluid velocity field. At the current low resolution mesh, the pressure variation next to each individual particle is unresolved and cannot be shown graphically. Moreover, the fluid velocity can only be expressed as accurately as its grid size. Therefore, this particle-fluid interaction force would be more accurately represented with more cells at the cost of increased computational time.

Conclusion

The project accuracy is currently limited to the conditions which is simulated in the code. The simulation time was practically limited to the computer on which the simulation was run. Seconds in real simulation time becomes dozens of hours of computational time. The time for the simulation to compile is heavily dependent on the complexity of each run. By increasing the number of particles through the particle density, the computational time increases significantly. As a result of satisfying the CFL condition to create valid results, significantly reduced time steps must be taken.

The code should be validated against experimental data or against computational journal articles that have verified their data experimentally. However, this was limited to the present geometry choice since it is difficult to quantitatively compare results for different applications. Qualitatively, the results agree with those analyzed in the literature review and with physical intuition.

The project contains a fundamental assumption that the theory performs accurately based on which the code and models are derived. The Navier Stokes equations used to solve the fluid breaks down when particles are in very close contact. In addition, the modeling of the particle forces is only as accurate as each model is accurate to the actual performance as determined experimentally.

The project has achieved a working and accurate representation of the fluidized bed problem. While only a few parameters were considered under this project, the problem will be expanded beyond the course. More complex models will include the mixing of multiple types of particles, and extending the problem into fully three dimensional simulation. The particle types can be selected from this binary system, spheres, or corn-shaped particles as considered by Ren. Likewise, the mixing of two types of initially-segregated particles can verify and compare the results achieved by Ren. These applications can be achieved in future developments extended through this project.

References

Allen, M.P., D. Frenkel, and J. Talbot. 1989. "Molecular dynamics simulation using hard particles". Computer Physics Reports. 9 (6): 301-353.

Beetstra, R., M.A. van der Hoef, and J.A.M. Kuipers. 2006. "A lattice-Boltzmann simulation study of the drag coefficient of clusters of spheres". Computers and Fluids. 35 (8-9): 966-970.

Capecelatro, J., O. Desjardins. An Euler-Lagrange strategy for simulating particle-laden flows, Journal of Computational Physics 238 (2013) 1–31.

Chhabra, R.P., L. Agarwal, and N.K. Sinha. 1999. "Drag on non-spherical particles: an evaluation of available methods". *Powder Technology*. 101 (3): 288-295.

Chien, S.-F. 1994. "Settling Velocity of Irregularly Shaped Particles". SPE Drilling and Completion (Society of Petroleum Engineers). 9 (4): 281.

Clift, R., John R. Grace, and Martin E. Weber. 1978. *Bubbles, drops, and particles*. New York: Academic Press.

Crowe, Clayton T. 2005. *Multiphase Flow Handbook*. Boca Raton: C R C Press LLC.

Desjardins, O., G. Blanquart, G. Balarac, H. Pitsch. High order conservative finite difference scheme for variable density low Mach number turbulent flows, Journal of Computational Physics 227 (2008) 7125–7159.

Donev A, R Connelly, FH Stillinger, and S Torquato. 2007. "Underconstrained jammed packings of nonspherical hard particles: ellipses and ellipsoids". Physical Review. E, Statistical, Nonlinear, and Soft Matter Physics. 75 (5).

Ganser, Gary H. 1993. "A rational approach to drag prediction of spherical and nonspherical particles". *Powder Technology*. 77 (2): 143-152.

Goossens, D. 1987. "A drag coefficient equation for natural, irregularly shaped particles". *Catena*. 14 (1): 73-99.

Hartman, M., O. Trnka, and K. Svoboda. 1994. "Free Settling of Nonspherical Particles". *Industrial & Engineering Chemistry Research*. 33 (8): 1979.

Hilton, J.E., L.R. Mason, and P.W. Cleary. 2010. "Dynamics of gas-solid fluidised beds with non-spherical particle geometry". Chemical Engineering Science. 65 (5): 1584-1596.

Hottovy, John D., and Nicholas D. Sylvester. 1979. "Drag Coefficients for Irregularly Shaped Particles". Industrial & Engineering Chemistry Process Design and Development. 18 (3): 433-436.

Lasso, I. A., and P. D. Weidman. 1986. "Stokes drag on hollow cylinders and conglomerates". *Physics of Fluids*. 29 (12): 3921.

Leith, David. 1987. "Drag on Nonspherical Objects". *Aerosol Science and Technology*. 6 (2): 153-161.

Loth, E. 2008. "Drag of non-spherical solid particles of regular and irregular shape". *Powder Technology*. 182 (3): 342-353.

Madhav, G Venu, and R P Chhabra. 1995. "Drag on non-spherical particles in viscous fluids". *International Journal of Mineral Processing*. 43 (1-2): 15.

Mando, M., and L. Rosendahl. 2010. "On the motion of non-spherical particles at high Reynolds number". *Powder Technology*. 202 (1-3): 1-13.

Ren, Bing, Wenqi Zhong, Baosheng Jin, Yingjuan Shao, and Zhulin Yuan. 2013. "Numerical simulation on the mixing behavior of corn-shaped particles in a spouted bed". Powder Technology. 234: 58-66.

Subramaniam, Shankar. 2013. "Lagrangian–Eulerian methods for multiphase flows". Progress in Energy and Combustion Science. 39 (2-3): 215-245.

Tran-Cong, Sabine, Michael Gay, and Efstathios E Michaelides. 2004. "Drag coefficients of irregularly shaped particles". Powder Technology. 139 (1): 21-32.

Zhong W.Q., Zhang Y., Jin B., and Zhang M. 2009. "Discrete element method simulation of cylinder-shaped particle flow in a gas-solid fluidized bed". Chemical Engineering and Technology. 32 (3): 386-391.

Zhou, Z.Y., D. Pinson, R.P. Zou, and A.B. Yu. 2011. "Discrete particle simulation of gas fluidization of ellipsoidal particles". Chemical Engineering Science. 66 (23): 6128-6145.